

Cell Division Orientation on Biospecific Peptide Gradients

Brian M. Lamb,[†] Wei Luo,^{†,‡} Sarbajeet Nagdas,[†] and Muhammad N. Yousaf^{*,†,‡}

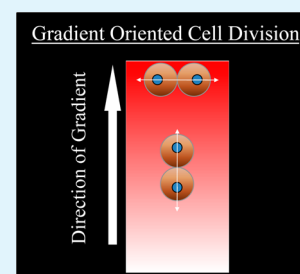
[†]Department of Chemistry, University of North Carolina at Chapel Hill, Chapel Hill, North Carolina 27599, United States

[‡]Department of Chemistry and Centre for Research on Biomolecular Interactions, York University, Toronto, Ontario M3J 1P3, Canada

S Supporting Information

ABSTRACT: An assay was developed for determining cell division orientation on gradients. The methodology is based on permeating microfluidic devices with alkanethiols and subsequent printing of cell adhesive peptide gradient self-assembled monolayers (SAMs) for examining oriented cell divisions. To our knowledge, there has been no study examining the correlation between cell division orientations based on an underlying ligand gradient. These results implicate an important role for how the extracellular matrix may control cell division. These surfaces would allow for a range of cell behavior (polarization, migration, division, differentiation) studies on tailored biospecific gradients and as a potential biotechnological platform to assess small molecule perturbations of cell function.

KEYWORDS: cell division, self-assembled monolayers, surface gradients, cell migration, cell polarization, cell orientation



INTRODUCTION

The correct cell migration and cell division orientation in space and time is essential for the proper function of a multicellular organism.^{1,2} During early embryonic development, cells experience a range of physicochemical and hydrodynamic forces,³ and they are continuously bombarded by soluble small molecules and gradients of morphogens.⁴ These cells also rely on cell–cell contacts and attachment to the extracellular matrix (ECM) to direct their movement for higher-order function.⁵ To establish an asymmetric environment, gradients of soluble morphogens and gradients of ligands on the ECM are thought to help guide and instruct cell movement.⁶ During cell migration, cells may also divide while experiencing these gradient microenvironments. It is not clear if during cell division the cells retain the gradient information, which directs their cell division orientation, or if the cells divide irrespective of the gradients and then re-establish polarization and migration post division. Recent research has shown that imposing geometric constraints on cells with micropatterned or nanopatterned ECM presenting surfaces effectively orient cell polarity and cell division.^{7–10} However, most cells in vivo experience soluble and/or surface gradients, and there has been no report or model substrate to study how gradients of immobilized (haptotactic) ligands influence cell division orientation.

Herein, we demonstrate a model substrate for assaying for cell division orientation induced by haptotactic gradients. Using biospecific arginylglycylaspartic acid (RGD) gradients on SAMs, the effects of cell adhesive gradients on cell division orientation were examined. These experiments demonstrated sequestration of geometric and gradient effects on cell adhesions and subsequent cell divisions. Furthermore, it is shown that an identical assay can be used to probe cell division behaviors of single cells and cells within confluent monolayers.

The methodology is applicable for studies of a wide range of cell behaviors (polarization, migration, division, differentiation) and can potentially serve as a biotechnological platform to assess various molecule perturbations of cell function.

RESULTS AND DISCUSSION

To study cell division orientation preferences, we employed a surface chemistry and microfluidic approach to generate chemoselective and biospecific ligand gradients. We used a previously published solute permeation and diffusion (SPREAD) technique to generate a gradient of alkanethiols within a polydimethylsiloxane (PDMS) microfluidic stamp that could then be transfer printed to a bare gold surface (Figure 1 and Supporting Information, Figure 1S).^{11,12} This methodology relies on alkanethiol permeation and diffusion into a PDMS microfluidic device to create chemical gradients that can be printed directly onto surfaces. Because of the ease of use, the method is especially amenable for biological assays of cell behavior due to its ease and versatility in producing biospecific gradients at the micrometer length scale. Briefly, a gradient self-assembled monolayer (SAM) was formed by permeating 11-amino-oxyundecanethiol (molecule 1, Supporting Information, Scheme S1) into a microfluidic stamp and transfer printing onto a bare gold surface, essentially creating on the surface a “snapshot” of the diffused alkanethiol concentrations within the PDMS device. Backfilling the remaining bare gold regions with a tetra(ethylene glycol)undecanethiol (molecule 2, or EG₄SH (Supporting Information, Scheme S1)) allows for the surfaces to be inert to nonspecific protein adsorption and cell attachment.¹³ The oxyamine-terminated SAMs could then be

Received: April 11, 2014

Accepted: June 30, 2014

Published: July 9, 2014

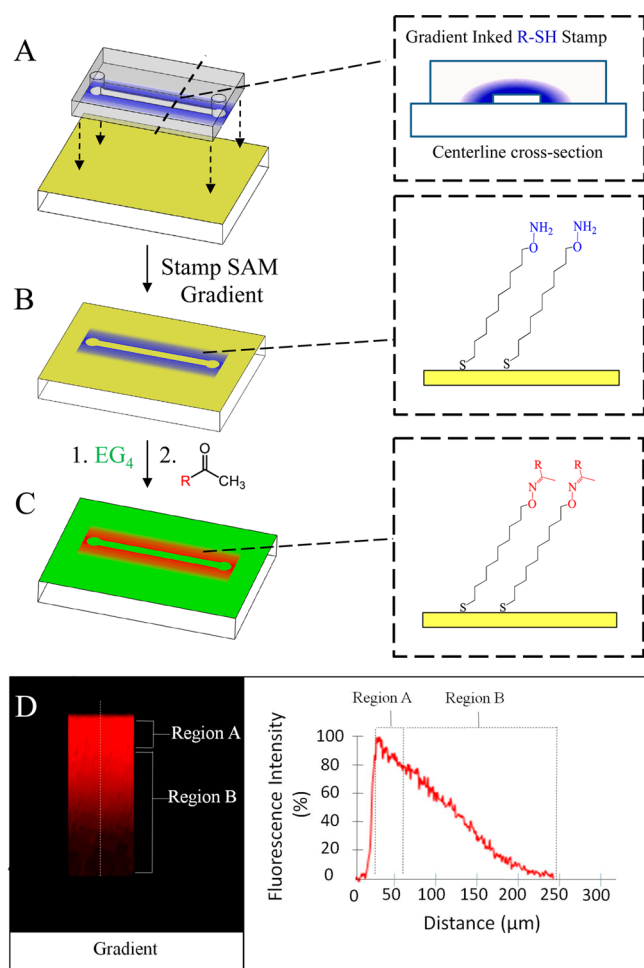


Figure 1. Fabrication of surface gradients presenting cell adhesive RGD peptide ligands. (A) Printing a stamp inked with (1) directly onto a gold substrate creates a gradient oxyamine-terminated SAM (B). (C) The remaining bare gold regions are backfilled with tetra(ethylene glycol) alkanethiol (EG₄SH) to form a SAM that is inert to nonspecific cell attachment. Addition of ketone-containing ligands results in the immobilization of ligands via an interfacial oxime linkage. (D) Characterization of a representative gradient generated by the SPREAD stamping method and reaction with a ketone-rhodamine. Fluorescence intensity profile of the SPREAD gradient on a gold surface showing a linear slope extending $\sim 200 \mu\text{m}$.

used to immobilize ligands or biomolecules containing ketone groups via an interfacial oxime linkage.¹⁴ Prior to cell experiments, the surface oxyamine-terminated gradient generated by the SPREAD technique was reacted with a ketone-containing RGD peptide (molecule 4, Supporting Information, Scheme S1) (10 mM, 3 h) to present RGD peptides at the surface-solution interface. The RGD sequence is found in the ECM protein fibronectin and is the minimum peptide sequence unit capable of binding integrin receptors to elicit biospecific cell adhesion and migration.¹⁵

Previous studies have shown that micro- and nanopatterned substrates are capable of orienting internal cellular machinery.⁸ However, many guidance cues in living organisms are dictated by soluble or surface-bound gradients.^{1–4} The differences between the micropatterned islands and gradients are profound.¹⁶ First, on single-cell patterns cells lack the ability to migrate in a particular direction. Although previous studies have provided quantitative analysis of the force-providing

mechanisms of cell division,⁹ these model substrates did not allow for the study of sustained orientation of cell behaviors during cell migration. Second, gradients provide guidance information, resulting in many complex behaviors directed toward a targeted location.^{17–19} Finally, gradients allow orientational freedom, and natural cell behavior can be observed with greater biological relevance.^{20–22}

Given the biological relevance of haptotactic gradients for directing cell orientation and function, it was sought to determine whether haptotactic (surface-bound guidance) gradients could influence cell division. Cell division orientation was assayed on $200 \mu\text{m}$ gradients for three key reasons. First, it was desired that the ratio of single cell size to gradient length range from 0.1 to 0.2 (cell size $20\text{--}40 \mu\text{m}$). This decision was made based on the RGD ligand density on the surface, which we calculated for these experiments to vary between 0 and 10% surface composition (A 1% surface density on a gold SAM surface is approximately 1.7×10^4 molecules/ μm^2). For cells experiencing the gradient of RGD ligands, this corresponds to a 1–2% RGD differential between the leading edge and the trailing edge of a migrating cell depending on its diameter. Second, gradients of approximately $200 \mu\text{m}$ in length are highly desired for experiments of haptotaxis.²³ Finally, the gradients printed with the SPREAD technique allow differentiation of geometric effects (caused by cell sampling pattern edge boundaries) from gradient effects (caused by anisotropic sampling of surface ligand density), to allow examination of cell behavior elicited solely by the gradients presented on the surface.

To confirm the haptotactic quality of the RGD peptide gradient we first studied the directional migration preference of adhered fibroblasts. It was observed that cells adhered to the RGD peptide gradient consistently migrated up the gradient toward the higher RGD density (Supporting Information, Figure S2). As controls, when the surface does not present RGD or has scrambled peptide (RDG) presented, cells do not adhere showing that the surface is inert to nonspecific cell attachment. A cell division orientation assay on gradients was performed as outlined in Figure 2. The behavior of a Rat 2 fibroblast cell line that simultaneously expresses mCherry modified histones and green fluorescent protein (GFP) α -tubulin was observed to enable live-cell fluorescence microscopy to reveal the dynamics of the cell nucleus and Golgi, respectively, during cell division (experimental setup was concluded in Supporting Information, Figure S3).²⁴ Upon data analysis, it was found that the orientation of the cell division axis in single cells was bimodal and strongly depended on a cell's position on the gradients (p value < 0.05). For ease of illustration, observed cell behaviors were grouped into regions A and B in Figure 3. Region A, within $40 \mu\text{m}$ of the top edge, is easy to identify, represents the highest ligand density, and ends abruptly (geometric edge). Region B, also readily identified, is beyond $40 \mu\text{m}$ and presents varying ligand density of a constant linear slope that ends asymptotically. Cell division orientation was determined by the nucleus–nucleus vector of the dividing Rat2 fibroblasts.

Figure 3 shows the cell division orientation vector histogram results for single cell in regions A and B of the gradient. On region A, cells were observed to migrate and elongate along the high density regions of the gradient. Resulting cell divisions exhibited a strong tendency to position the resulting nucleus–nucleus vector along an identical ligand density during cell division. This result supports previous findings in which cells

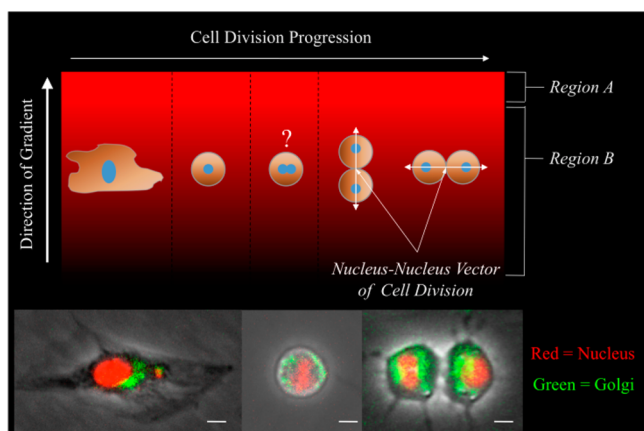


Figure 2. Experimental assay for determining single cell orientation of cell division preference on a gradient. (top) Cartoon showing a single cell migrating on a gradient and then undergoing division. The nucleus–nucleus vector of cell division on region A (higher density) and region B (lower density) is determined by time-lapse microscopy and compared to the direction of the underlying gradient. (bottom) Overlay images of a Rat2 cell undergoing cell division where the nucleus and Golgi are fluorescently stained to observe the plane of cell division. Scale bar represents 10 μm .

stretched onto cell adhesive regions oriented their cell division axis perpendicular to the longest side of the cell.⁷ Our observations validate these previous observations and further indicate cells have a strong preference to optimize their adhesion on the highest density RGD regions, which guides their cell division orientation. Although we initially expected that the direction of polarity would correlate with the orientation of cell division, we found the orientation of the nucleus–nucleus cell division vector on the gradient surfaces to be the key factor for determining the position of the two daughter cells. Although it will not be described further in this manuscript, we observed that cell polarity generally diminishes as a cell begins mitosis and eventually becomes more established along the cell division axis, as described by They et al.⁷

A better indication of how the underlying surface gradient regulates cell behavior is to examine cells exposed to gradient regions of identical slope and lacking a geometric edge. Cells in region B exhibited a preference to divide parallel to the direction of the gradient. Cells in this region do not experience any geometric boundaries but only differences in ligand density on the gradient surfaces. To ensure this behavior was a result of the underlying surface gradient, cell division orientations were also observed on uniform 200 $\mu\text{m} \times 5 \text{ cm}$ patterns (no gradient) presenting RGD peptide or fibronectin (p value < 0.05). The cells had random cell division orientation in both regions A and B. Furthermore, fibroblasts with focal adhesion kinase knocked out (FAK $-/-$ an important enzyme responsible for forming focal adhesions) showed random cell division orientation on the gradient.²⁵ These results suggest that the cell is strongly influenced by the information on the underlying gradient, mediated by integrin receptors, throughout cell division and cytokinesis.

The navigational information provided to cells by haptotactic gradients in vivo is convoluted by many adhesions with neighboring cells. The impact of these adhesions on overall cell behavior in the context of a gradient ECM has been overlooked, mainly due to a focus on single-cell behavior.^{26,27}

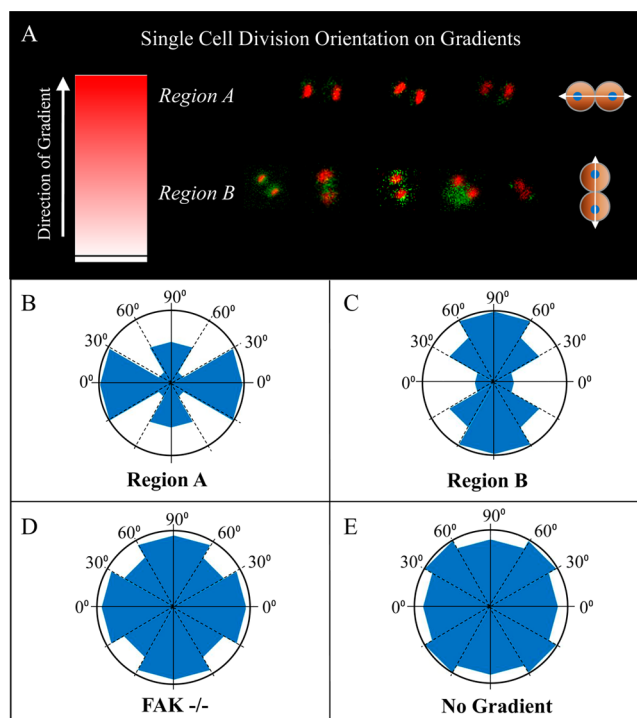


Figure 3. Orientation of single cells undergoing cell division on cell adhesive RGD peptide gradients. (A) Observed cells undergoing cell division in region A and region B of the gradient. Cells divide perpendicular to the gradient in region A and parallel to the gradient in region B. (bottom) Vector histograms of cell division orientation. (B) Cells divide perpendicular to the gradient in region A ($n = 43$). (C) Cells divide parallel to the gradient in region B ($n = 78$). (D) A FAK null cell line that is lack of focal adhesion kinase shows no preference of cell division on region A or B ($n = 51$). (E) With a uniform presentation of RGD peptides (no gradient), the Rat2 cells show random orientation of cell division ($n = 35$). Scale bar represents 30 μm .

Because of this precedent and the convenience of the methodology for assaying single cell behavior on gradients, it was sought to study and compare the interplay of cell–cell interactions and cell–material interactions for determining individual cell division orientations in confluent cell monolayers (Figure 4).

Rather than seeding cells at a low density for single-cell observation, cells were seeded onto the gradient surfaces to confluency, and then cell division orientations were quantified and grouped depending on the position on the gradient. Interesting results were observed for which we have seen no prior precedent. It was observed that cells in region A exhibit a nearly exclusive preference to orient the nucleus–nucleus vector axis perpendicular to the direction of the gradient. Cells in region B, however, did not show any orientation preference during cell division. It was hypothesized that this result may be due to cell crowding on the micropatterned gradients, and therefore a control experiment was performed in which confluent cell monolayers were patterned on uniform RGD or fibronectin surfaces (no gradient) of identical dimensions (5 cm \times 200 μm). On the uniform surfaces, cells oriented their cell division exclusively along the longest axis of the pattern, demonstrating that micropatterned dimensions exponentially larger than a single cell can influence cell division orientation. On uniform surfaces, single cells would be unable to sense the geometric restrictions (5 cm length vs 40 μm cell), but

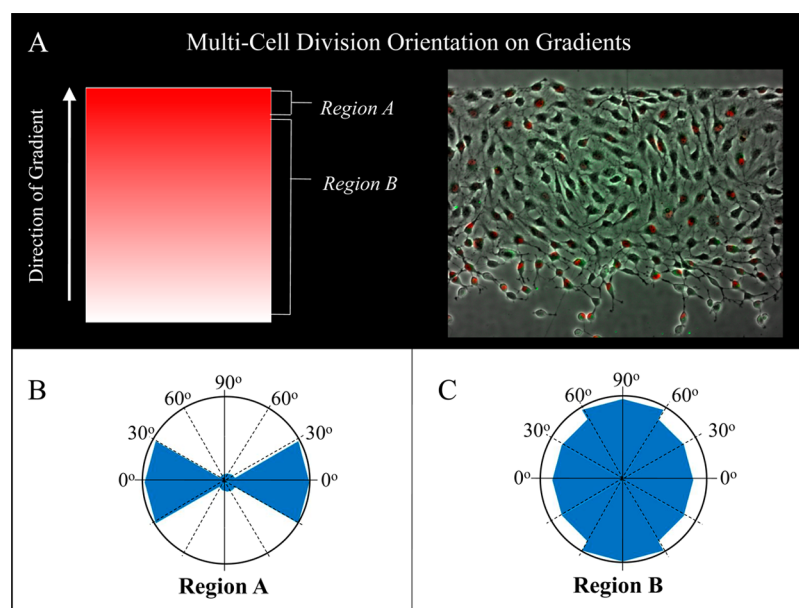


Figure 4. Cell division orientation as part of a confluent monolayer of cells on a gradient. (top) Cartoon of the gradient and overlay image of a confluent layer of cells on the gradient ($200\ \mu\text{m}$ gradient \times $5\ \text{cm}$ pattern width). (A) Cell division orientation on region A is perpendicular to the gradient ($n = 35$). (B) Cell division orientation is random in region B ($n = 81$). (C) Cell division orientation on uniform $200\ \mu\text{m} \times 5\ \text{cm}$ patterns ($n = 63$). Scale bar represents $50\ \mu\text{m}$.

collectively a confluent monolayer experiences a type of crowding stress that induces cells to reorient and accommodate to their environment.

These results suggest that cell–cell contacts allow cells to communicate or redirect mechanical stress experienced by a monolayer, or cellular tissue, as a group. A possible explanation for the experimental observation that cell division orientation is lost in region B of the gradients may be due to the asymptotic region of the cell adhesive gradients. It was observed on gradients, in which ligand density terminates asymptotically, that individual cells actively attempt to migrate toward lower RGD density regions where fewer cells are present. Cells in these regions are essentially forced off of the patterning regions, potentially alleviating stresses from higher density regions of the gradient. The data obtained by observation of cell division orientation in region A also supports this hypothesis, since the highest density of RGD and thus optimal surface adhesion is possible in this area. Cell–cell interactions allow the cells to remain connected to each other, thereby permitting them to distribute the crowding stress to all cells confined on the micropattern. The asymptotic loss of ligand density in region B, therefore, serves to alleviate this crowding stress, since no abrupt boundaries are present. Furthermore, it is hypothesized that the observed effects inhibit geometric constraints from influencing cell division orientation. The results especially indicate the effect is due to direct contact rather than paracrine signaling, especially by the differences in cell division orientation in regions A and B of the gradient. Paracrine signaling would be identical across both of these regions, whereas remarkable differences are observed between the control and gradient experiments. Finally, the results we observed for cell division orientation on gradients is comparable to those obtained by a traditional wound healing assay.

CONCLUSION

The cell division orientation experiments presented herein illustrate the effects of underlying cell adhesive surface gradients on cell division orientation, an important process involved in complex biological transformations of embryonic tissues into a viable organism. Single cells on large gradients are allowed 360 degrees of orientation possibilities, yet during cell division they show strong preferences to orient their cell division axis based on their location on a gradient. To our knowledge, no study of cell division orientation preference of cells in confluent monolayers has been reported, and our results demonstrate unique cellular behaviors in response to gradients. These results are important for future cell-based material research in many fields due to the central role of wound repair and developmental biology for proper organism function and survival. The effects of gradients on cells with many bordering contacts remains an unexplored area for future research. The results of this study demonstrate how a single cell of less than $40\ \mu\text{m}$ in total diameter can be influenced by patterns exponentially larger in width and length. The observation that gradients alleviate observed cell division patterns in confluent monolayers on uniform patterns draws a parallel between gradients and standard wound healing assays. Although it is expected that perturbing cell–cell adhesions would influence the resulting cell behaviors, further analysis is required especially in analyzing the influence of different coculture cell types, which may act as leading cells in this process. Further studies will also explore the role of paracrine signaling in influencing cell division orientation.

EXPERIMENTAL SECTION

Synthesis of Alkanethiols and Ketone-Functionalized Rhodamine. Tetra(ethylene-glycol)undecanethiol (2, EG_4SH) was synthesized as reported previously.¹³ 11-Amino-oxyundecanethiol (1, oxyamine–alkanethiol) and ketone-functionalized rhodamine were synthesized according to Park et al.¹⁴

Solid-Phase Peptide Synthesis of RGD (4). Ketone-functionalized GRGDS (RGD) peptide was synthesized using a peptide synthesizer (CS Bio) at a 0.1 mmol scale. 4-acetylbutyric acid was used without protection to provide the ketone functional group. The peptide was obtained from the resin after treatment with 10 mL of trifluoroacetic acid (TFA) containing 5% water and 5% methylene chloride for 2 h under bubbling nitrogen followed by filtration. The filtrate was mixed with diethyl ether (40 mL), and the mixture was centrifuged at 3000 rpm for 15 min to afford a white precipitate. The precipitate was lyophilized overnight to obtain a white solid. Electrospray ionization (ESI) GRGDS-mass calcd 714.4; found 714.3.

Microfabrication. The microfluidic cassettes were fabricated using soft lithography.²⁸ Patterns were designed using masks drawn in Adobe Illustrator CS3 and photoplotted by Pageworks (NH, USA) onto transparencies. These masks were then used to pattern SU-8 50 (Microchem) using the manufacturer's directions to obtain 50 μm channel depth. Sylgard 184 (Dow Corning) was cast onto the mold in a 1:10 ratio of curing agent to elastomer w/w. The prepolymer was degassed for 15 min and then poured over the mold. The prepolymer was cured for 1 h at 75 °C. The PDMS was removed from the master, and microfluidic access holes were punched into the PDMS to allow fluid flow.

Preparation of Gold-Coated Substrates. Gold substrates were prepared by electron beam deposition of first titanium (6 nm) and then gold (24 nm) on 24 \times 100 mm glass microscope slides. The slides were cut into 1 \times 5 cm² pieces and washed with absolute ethanol before use.

PDMS Cleansing. Prior to use, all newly fabricated PDMS microfluidic cassettes were Soxhlet extracted with ethyl acetate for 6 h.²⁹ After each use, the stamps were immersed in CH₂Cl₂ (DCM) overnight to extract remaining thiol absorbed in the PDMS, then dried in a vacuum chamber for 2 h.

SPREAD Inking and Printing Procedure. A clean PDMS microfluidic stamp was reversibly sealed onto a glass microscope slide. A solution of 5 mM oxyamine–alkanethiol in ethanol was flowed into a microfluidic stamp, and the static solution was allowed to permeate the microchannels for 60 s. The cassette was then evacuated with the aid of negative pressure, and the alkanethiol was allowed to diffuse into the PDMS (5 min diffusion time). After diffusion, the PDMS cassette was removed from the glass surface and pressed onto a gold surface for 5 s. After printing, the surface was immersed in 1 mM EG₄SH solution to make the surface inert to nonspecific cell attachment.

Fluorescence Visualization. The surfaces were reacted with a fluorescent ketone-functionalized rhodamine (molecule 3 of the Supporting Information, Scheme S1, 10 mM, 3 h) and characterized by fluorescence microscopy.¹⁴ Fluorescence images were taken using a Nikon Eclipse TE2000-E inverted microscope (Nikon USA, Inc., Melville, NY), and the data were analyzed by metamorph software.

RGD Ketone Functionalization of Gradient Surfaces. Surfaces were exposed to solutions of 10 mM RGD for 3 h and then rinsed thoroughly with water and dried with a stream of N₂.

Cell Culture. Rat2 fibroblasts with mCherry labeled histone and GFP labeled Golgi were prepared and handled according to Uetchrect.²⁴ The cells were cultured in Dulbecco's Modified Eagle Medium (Gibco) containing 5% fetal bovine serum and 1% penicillin/streptomycin. Cells were removed with a solution of 0.05% trypsin in 0.53 mM ethylenediaminetetraacetic acid, resuspended in serum-free medium (100 000 cells/mL) for cell seeding, and allowed 2 h to attach to the surface prior to the addition of serum-containing media. Confluent cell monolayer studies were initiated 12 h after seeding. For passage, cells were resuspended in the same 10 mL of medium that they were growing in, and 3 mL was transferred to 7 mL of fresh medium in a new flask.

Cell Staining and Microscopy.³⁰ Time-lapse microscopy was performed by inverting cell-seeded substrates onto a Petri dish prior to fluorescence imaging for 12–24 h (Supporting Information, Figure 2). A mixture of grease and 25 μm diameter microspheres are applied to the corners of the patterned substrate prior to placement directly on top of a Petri dish, serving as the imaging chamber (Supporting Information, Figure 3).³¹ Cells remained healthy during the entirety of

the microscopy acquisition period, and were able to divide and migrate. Fluorescence images were taken using a Nikon Eclipse TE2000-E inverted microscope (Nikon USA, Inc., Melville, NY), and the data were analyzed by metamorph software.

■ ASSOCIATED CONTENT

● Supporting Information

Detailed materials and methods section, list of molecules used, SPREAD technique diagram, inverted microscopy setup. This material is available free of charge via the Internet at <http://pubs.acs.org/>.

■ AUTHOR INFORMATION

Corresponding Author

*E-mail: chrchem@yorku.ca. Phone: 416-736-2100 ext. 77718. Fax: 416-736-5512.

Notes

The authors declare no competing financial interest.

■ ACKNOWLEDGMENTS

This work was supported by the Carolina Center for Cancer Nanotechnology Excellence (NCI), The Burroughs Wellcome Foundation (Interface Career Award), The National Science Foundation (Career Award), National Science and Engineering Research Council of Canada (NSERC), and the Canadian Foundation for Innovation (CFI).

■ REFERENCES

- (1) Wong, K.; Park, H. T.; Wu, J. Y.; Rao, Y. Slit Proteins: Molecular Guidance Cues for Cells Ranging from Neurons to Leukocytes. *Curr. Opin. Genet. Dev.* **2002**, *12*, 583–591.
- (2) Schmid, R. S.; Shelton, S.; Stanco, A.; Yokota, Y.; Kreidberg, J. A.; Anton, E. S. Alpha 3 beta 1 Integrin Modulates Neuronal Migration and Placement During Early Stages of Cerebral Cortical Development. *Development* **2004**, *131*, 6023–6031.
- (3) Engler, A. J.; Sen, S.; Sweeney, H. L.; Discher, D. E. Matrix Elasticity Directs Stem Cell Lineage Specification. *Cell* **2006**, *126*, 677–689.
- (4) Ridley, A. J.; Schwartz, M. A.; Burridge, K.; Firtel, R. A.; Ginsberg, M. H.; Borisy, G.; Parsons, J. T.; Horwitz, A. R. Cell Migration: Integrating Signals from Front to Back. *Science* **2003**, *302*, 1704–1709.
- (5) Izaguirre, J. A.; Chaturvedi, R.; Huang, C.; Cickovski, T.; Coffland, J.; Thomas, G.; Forgacs, G.; Alber, M.; Hentschel, G.; Newman, S. A.; Glazier, J. A. CompuCell, a Multi-Model Framework for Simulation of Morphogenesis. *Bioinformatics* **2004**, *20*, 1129–1137.
- (6) Kutejova, E.; Briscoe, J.; Kicheva, A. Temporal Dynamics of Patterning by Morphogen Gradients. *Curr. Opin. Genet. Dev.* **2009**, *19*, 315–322.
- (7) Thery, M.; Racine, V.; Pepin, A.; Piel, M.; Chen, Y.; Sibarita, J. B.; Bornens, M. The Extracellular Matrix Guides the Orientation of the Cell Division Axis. *Nat. Cell Biol.* **2005**, *7*, 947–953.
- (8) Santos, M. I.; Tuzlakoglu, K.; Fuchs, S.; Gomes, M. E.; Peters, K.; Unger, R. E.; Piskin, E.; Reis, R. L.; Kirkpatrick, C. J. Endothelial Cell Colonization and Angiogenic Potential of Combined Nano- and Micro-fibrous Scaffolds for Bone Tissue Engineering. *Biomaterials* **2008**, *29*, 4306–4313.
- (9) Diaz, C.; Schilardi, P. L.; Salvarezza, R. C.; de Mele, M. F. Nano/Microscale Order Affects the Early Stages of Biofilm Formation on Metal Surfaces. *Langmuir* **2007**, *23*, 11206–11210.
- (10) Idota, N.; Tsukahara, T.; Sato, K.; Okano, T.; Kitamori, T. The use of Electron Beam Lithographic Graft-polymerization on Thermoresponsive Polymers for Regulating the Directionality of Cell Attachment and Detachment. *Biomaterials* **2009**, *30*, 2095–2101.
- (11) Lamb, B. M.; Barrett, D. G.; Westcott, N. P.; Yousaf, M. N. Microfluidic Lithography of SAMs on Gold to Create Dynamic

Surfaces for Directed Cell Migration and Contiguous Cell Cocultures. *Langmuir* **2008**, *24*, 8885–8889.

(12) Lamb, B. M.; Park, S.; Yousaf, M. N. Microfluidic Permeation Printing of Self-Assembled Monolayer Gradients on Surfaces for Chemoselective Ligand Immobilization Applied to Cell Adhesion and Polarization. *Langmuir* **2010**, *26*, 12817–12823.

(13) Luo, W.; Westcott, N. P.; Pulsipher, A.; Yousaf, M. N. Renewable and Optically Transparent Electroactive Indium Tin Oxide Surfaces for Chemoselective Ligand Immobilization and Biospecific Cell Adhesion. *Langmuir* **2008**, *24*, 13096–13101.

(14) Park, S.; Yousaf, M. N. An Interfacial Oxime Reaction to Immobilize Ligands and Cells in Patterns and Gradients to Photo-Active Surfaces. *Langmuir* **2008**, *24*, 6201–6207.

(15) Pierschbacher, M. D.; Ruoslahti, E. Cell Attachment Activity of Fibronectin can be Duplicated by Small Synthetic Fragments of the Molecule. *Nature* **1984**, *309*, 30–33.

(16) Genzer, J.; Bhat, R. R. Surface-bound Soft Matter Gradients. *Langmuir* **2008**, *24*, 2294–2317.

(17) Wells, N.; Baxter, M. A.; Turnbull, J. E.; Murray, P.; Edgar, D.; Parry, K. L.; Steele, D. A.; Short, R. D. The Geometric Control of E14 and R1Mouse Embryonic Stem Cell Pluripotency by Plasma Polymer Surface Chemical Gradients. *Biomaterials* **2009**, *30*, 1066–1070.

(18) Pei, J.; Hall, H.; Spencer, N. D. The Role of Plasma Proteins in Cell Adhesion to PEG Surface-Density-Gradient-Modified Titanium Oxide. *Biomaterials* **2011**, *32*, 8968–8978.

(19) Smith, J. T.; Tomfohr, J. K.; Wells, M. C.; Beebe, T. P.; Kepler, T. B.; Reichert, W. M. Measurement of Cell Migration on Surface-bound Fibronectin Gradients. *Langmuir* **2004**, *20*, 8279–8286.

(20) Zhang, K. C.; Sugawara, A.; Tirrell, D. A. Generation of Surface-Bound Multicomponent Protein Gradients. *ChemBioChem* **2009**, *10*, 2617–2619.

(21) Lin, X. K.; He, Q.; Li, J. B. Complex Polymer Brush Gradients Based on Nanolithography and Surface-initiated Polymerization. *Chem. Soc. Rev.* **2012**, *41*, 3584–3593.

(22) Simon, C. G.; Lin-Gibson, S. Combinatorial and High-Throughput Screening of Biomaterials. *Adv. Mater.* **2011**, *23*, 369–387.

(23) Love, J. C.; Estroff, L. A.; Kriebel, J. K.; Nuzzo, R. G.; Whitesides, G. M. Self-assembled Monolayers of Thiolates on Metals as a Form of Nanotechnology. *Chem. Rev.* **2005**, *105*, 1103–1169.

(24) Uetrecht, A. C.; Bear, J. E. Golgi Polarity does not Correlate with Speed or Persistence of Freely Migrating Fibroblasts. *Eur. J. Cell Biol.* **2009**, *88*, 711–717.

(25) Ilc, D.; Furuta, Y.; Kanazawa, S.; Takeda, N.; Sobue, K.; Nakatsuji, N.; Nomura, S.; Fujimoto, J.; Okada, M.; Yamamoto, T. Reduced Cell Motility and Enhanced Focal Adhesion Contact Formation in Cells from FAK-Deficient Mice. *Nature* **1995**, *377*, 539–544.

(26) Gierasch, L. M.; Gershenson, A. Post-Reductionist Protein Science, or Putting Humpty Dumpty Back Together Again. *Nat. Chem. Biol.* **2009**, *5*, 774–777.

(27) Lechler, T.; Fuchs, E. Asymmetric Cell Divisions Promote Stratification and Differentiation of Mammalian Skin. *Nature* **2005**, *437*, 275–280.

(28) Deng, T.; Tien, J.; Xu, B.; Whitesides, G. M. Using Patterns in Microfiche as Photomasks in 10- μ m-Scale Microfabrication. *Langmuir* **1999**, *15*, 6575–6581.

(29) Thibault, C.; Severac, C.; Mingotaud, A. F.; Vieu, C.; Mauzac, M. Poly(dimethylsiloxane) Contamination in Microcontact Printing and its Influence on Patterning Oligonucleotides. *Langmuir* **2007**, *23*, 10706–10714.

(30) Hoover, D. K.; Chan, E. W. L.; Yousaf, M. N. Asymmetric Peptide Nanoarray Surfaces for Studies of Single Cell Polarization. *J. Am. Chem. Soc.* **2008**, *130*, 3280–3281.

(31) Hodgson, L.; Chan, E. W. L.; Hahn, K. M.; Yousaf, M. N. Combining Surface Chemistry with a FRET-based Biosensor to Study the Dynamics of RhoA GTPase Activation in Cells on Patterned Substrates. *J. Am. Chem. Soc.* **2007**, *129*, 9264–9265.